CHEMICAL STATE AND ELEMENTAL DISTRIBUTION OF METAL IMPURITIES IN POLYCRYSTALLINE SILICON SOLAR CELLS

S.A. McHugo[1,2], G. Lamble[1], A.C. Thompson[2], I. Perichaud[3] and S. Martinuzzi[3]

[1]Advanced Light Source Division, Lawrence Berkeley National Laboratory, University of California, Berkeley, CA, 94720 USA
[1]Center for X-ray Optics, Materials Science Division, Lawrence Berkeley National Laboratory, University of California, Berkeley, CA, 94720 USA
[3]Lab. de Photoélectricité des Semi-Conducteurs, University of Marseille, FRANCE

ABSTRACT

The work presented here directly measures the chemical state and elemental distributions of metal impurities in polycrystalline silicon used for terrestrial-based solar cells. The goal of this project was to determine if a correlation exists between poorly performing regions of solar cells and metal impurity distributions as well as to ascertain the chemical state of the impurities. Synchrotron-based x-ray fluorescence mapping and x-ray absorption spectroscopy, both with a spatial resolution of $1\mu m^2$, were used to measure impurity distributions and chemical state, respectively, in poorly performing regions of polycrystalline silicon. The Light Beam Induced Current method was used to measure minority carrier recombination in the material in order to identify poor performance regions. We have detected iron, chromium and nickel impurity precipitates and we have recognized a direct correlation between impurity distributions and poor performing regions in both as-grown and fully processed material. Furthermore, we have results, which indicate that the Fe in the polysilicon material is in oxide form, not a silicide form. These results provide a fundamental understanding into the efficiency-limiting factors of polycrystalline silicon solar cells as well as yielding insight for methods of solar cell improvement.

INTRODUCTION

Polycrystalline silicon can be used to fabricate solar cells with a moderate solar conversion efficiency and low fabrication costs. Although these cells are presently manufactured for terrestrial-based applications, an improvement in the efficiency of these cells would greatly increase their commercial viability. Presently, polycrystalline solar cells have efficiencies of 13-15% as compared to more expensive, single crystalline solar cells with efficiencies of 17-20% [1]. The primary cause for lowered efficiencies is localized regions of high minority carrier recombination, which possess high concentrations of dislocations [2-4]. However, it is known that minority carrier recombination at "clean" dislocations is relatively weak but greatly increases by decoration or precipitation of transition metal impurities [5-8]. This suggests the dislocations in high recombination regions of polycrystalline silicon are decorated with transition metals. Past work, [9], has provided indirect evidence that metal impurities are precipitated in regions of high carrier recombination while other work, [10], has revealed metal impurity agglomerations at dislocations in polycrystalline silicon. However, no direct evidence has been provided to relate high minority carrier recombination with transition metals in this material. In fact, carbon or oxygen may play an important role since these impurities are found in high concentrations in most polycrystalline silicon materials, $\approx 10^{18}$ atoms/cm^3.

The first *direct* evidence of a relationship between metal impurities and poor performance is provided in this work and has recently been published [11]. In this work, we have performed mapping of metal impurity distributions using the x-ray fluorescence microprobe, beamline

10.3.1 at the Advanced Light Source (ALS), with which we have obtained a direct correlation between metal impurities, such as Fe, Cr and Ni, and poor performance regions of the material. Additionally, we have results on the chemical state of Fe in this material, specifically the Fe is in the form of an oxide, not a silicide. These results have serious implications in regards to strategies for material improvement.

EXPERIMENT

Boron doped polycrystalline silicon grown by an electromagnetic casting method [12] was used in this study. In order to locate poor performance regions, minority carrier recombination was mapped across the as-grown material with the Light Beam Induced Current (LBIC) method, using 880nm wavelength light. The frontside of the samples were analyzed using synchrotron-based x-ray fluorescence (XRF) mapping in order to determine metal impurity content and distribution. The XRF equipment is located at the microprobe beamline, 10.3.1, in the ALS. It uses 12.5keV monochromatic radiation to excite elements in the sample with a spatial resolution of $1\mu m^2$ and a Si-Li detector to measure fluorescence x-rays from the sample, all in atmospheric conditions. The XRF microprobe sensitivity is impurity and matrix specific but, for example, the system can detect a single Fe or Cu precipitate/agglomerate in silicon greater than 10-20nm in radius. The sampling depth for 3d transition metal impurities in silicon is approximately 50μm. It should be noted that the sensitivity of the microprobe drops considerably for elements with an atomic number < 16. X-ray absorption studies were carried out at beamline 10.3.2 in the ALS. A four crystal Si monochromator produces a tunable monochromatic x-ray beam, which is focussed to a $1\mu m^2$ spot with a pair of grazing incidence mirrors. A Si-Li detector was used to detect fluorescence x-rays and quantify absorption for specific elements. Detail of the absorption apparatus is given in [13].

RESULTS AND DISCUSSION

LBIC mapping of minority carrier recombination across the polycrystalline silicon sample revealed localized regions of high carrier recombination. A typical LBIC map in a portion of the cast polysilicon is shown in Figure 1 where dark regions indicate areas of high carrier recombination. Note the regions of high recombination located approximately in the center of the LBIC scan area.

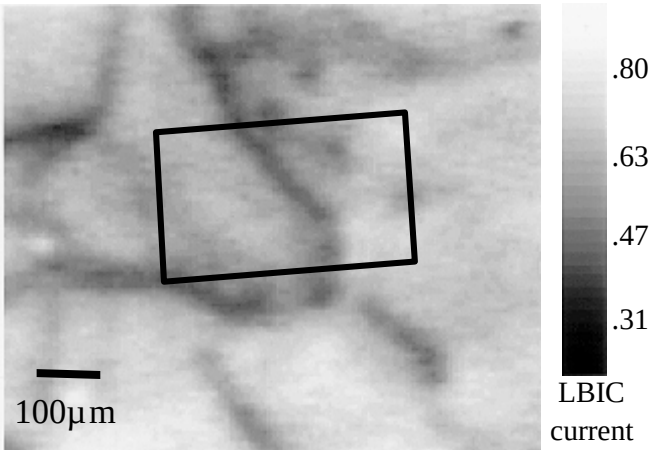

Figure 1: Light Beam Induced Current map of carrier recombination across a portion of multicrystalline silicon. Dark regions indicate high carrier recombination. The black box denotes the area analyzed with x-ray fluorescence.

X-ray Fluorescence (XRF) spectra were taken at $1\mu m^2$ points in the region of Figure 1 as denoted by the black box. No impurity-generated x-ray fluorescent radiation was detected in regions of low minority carrier recombination. However, x-ray fluorescent radiation associated with Cr, Fe and Ni was detected in regions of high carrier recombination. Concentrations of impurities at each $1\mu m^2$ spot were calculated by data analysis of the collected spectra and comparison to standard samples with known concentrations of impurities. Impurity maps were produced in the region denoted by the black box in Figure 1. Figure 2 is an impurity map of Fe in this region. Maps of Ni and Cr revealed the exact same distribution as the Fe, indicating a preferred precipitation site exists for these impurities. By comparison of Figures 1

and 2, one can clearly see a correlation between metal impurity distributions and minority carrier recombination. These results indicate metal impurities are the cause for high carrier recombination regions in polycrystalline silicon and, therefore, play a significant role in the performance of the material as a solar cell.

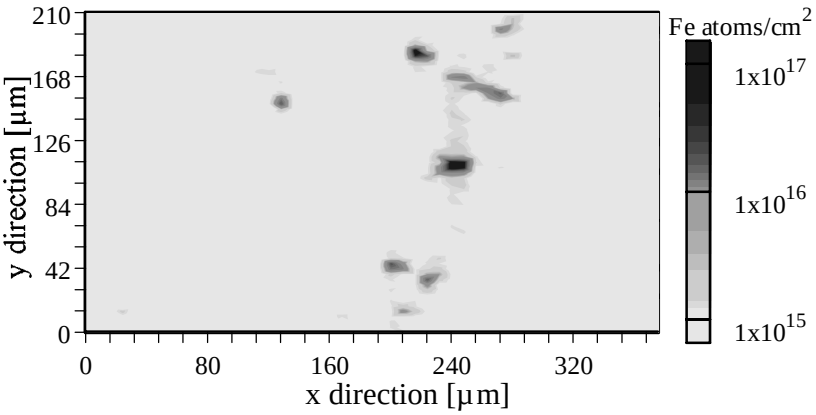

Figure 2: Fe distribution in polycrystalline silicon. The mapped area directly corresponds to the area in the black box of Figure 1. Note the correlation between metal impurity distributions and carrier recombination.

At each high impurity content region of Figure 2, a single precipitate or a number of precipitates may reside in each $1\mu m^2$ spot. If only one precipitate is assumed present, the diameter can be calculated from the measured impurity concentrations and assuming the precipitate is located at or near the surface. For instance, the measured concentration of $5x10^{16}$ atoms/cm^2 for Fe shown in Figure 2 would suggest one precipitate with a diameter of 288nm is present in that area. However, considering earlier work [10,14], the impurities in Figure 2 are more likely a fine dispersion of smaller impurity precipitates.

We have also performed x-ray absorption studies on this polysilicon material. Spectra were taken with a $1\mu m^2$ spot on regions of high Fe content. A summation of spectral scans at the Fe K absorption edge was taken in the Fe-rich region of Figure 2, as shown in Figure 3. Additionally, for purpose of comparison, we also provide the summed spectrum of a standard sample of an elemental Fe film and a α-Fe_2O_3 powder. The elemental Fe standard has a body centered cubic crystal symmetry while the α-Fe_2O_3 standard has a hexagonal crystal symmetry with the Fe in a +3 charge-state. The spectra shapes of the Fe in polysilicon and Fe in α-Fe_2O_3 are closely matched, especially in the near edge region, indicating the Fe in polysilicon has a similar symmetry as α-Fe_2O_3. Both of these absorption spectra are significantly different than the Fe film standard. Considering iron silicide is in either a cubic, tetragonal or orthorhombic crystal symmetry while α-Fe_2O_3 possesses a hexagonal crystal symmetry, the absorption spectra of iron silicides would be significantly different than the spectra obtained for Fe in polysilicon. Therefore, our results indicate the Fe in the polysilicon is not in an iron silicide state but rather in an oxide state. Further work is planned to produce iron silicide standards (FeSi and $FeSi_2$) for direct comparison of x-ray absorption spectra.

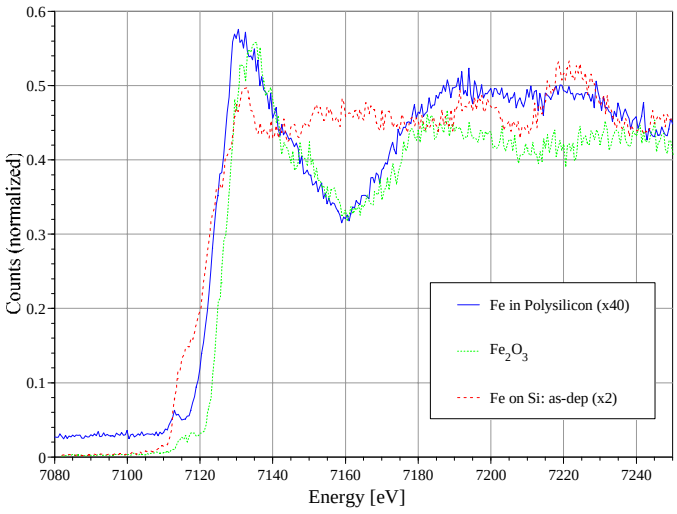

Figure 3: X-ray absorption spectroscopy of Fe in polysilicon, Fe in Fe_2O_3 and elemental Fe. Note the similarity between the Fe in polysilicon and Fe in Fe_2O_3.

The chemical state of metals in polysilicon drastically alters the removal of impurities from the material and, in turn, improvements in performance. For example, the binding energy of a Fe atom to a Fe oxide phase is drastically higher than a Fe iron to a Fe silicide phase, [15]. This constitutes a lower concentration of dissolved Fe impurities in the presence of a Fe oxide particle as compared to a Fe silicide particle during an annealing treatment. This lower concentration would decrease the flux of impurities out of the material during impurity removal and severely hinder material improvement. For instance, a 20nm diameter precipitate of $FeSi_2$ in silicon would require minutes to hours for complete dissolution at moderate temperatures while a precipitate of the same size of α-Fe_2O_3 would require days to weeks to fully dissolve. Therefore, the identification of Fe oxide in polycrystalline silicon indicates improvement of polysilicon solar cells is an arduous task and perhaps preventative measures are required.

CONCLUSIONS

In summation, metal impurities were found in polycrystalline silicon used for solar cells. The distribution of impurities correlated directly with poor performing regions of the material. These results are the first direct proof that metal impurities significantly affect the performance of polycrystalline silicon solar cells. Furthermore, our results indicate that the chemical state of Fe in this material is Fe oxide rather than the expected Fe silicide. This is the first indication that impurity removal from silicon is severely limited by the chemical state of the impurity precipitate.

ACKNOWLEDGMENTS

The authors would like to thank B. Gunion, R. Tackaberry, R. Celestre and A. MacDowell for their work on beamlines 10.3.1 and 10.3.2.

REFERENCES

1. J. M. Gee, R. R. King and K. W. Mitchell, 25th IEEE Photovoltaic Specialists Conference, Washington D.C., pg. 409, (1996)
2. S. Pizzini, A. Sandrinelli, M. Beghi, D. Narducci, F. Allegretti, S. Torchio, G. Fabbri, G. P. Ottaviani, F. Demartin and A. Fusi, *J. Electrochem. Soc.* **135**, 155, (1988)
3. B. L. Sopori, L. Jastrzebski, T. Tan and S. Narayanan, 12th European Photovoltaic Solar Energy Conference, Netherlands, 1003, (1994)
4. S. A. McHugo, H. Hieslmair and E. R. Weber, *Appl. Phys. A.* **64**, 127, (1997)
5. C. Cabanel and J. Y. Laval, *J. Appl. Phys.* **67**, 1425, (1990)
6. T. S. Fell, P. R. Wilshaw and M. D. d. Coteau, *Phys. Stat. Sol. (a).* **138**, 695, (1993)
7. V. Higgs and M. Kittler, *Appl. Phys. Lett.* **63**, 2085, (1993)
8. M. Kittler, W. Seifert and V. Higgs, *Phys. Stat. Sol. (a).* **137**, 327, (1993)
9. L. Jastrzebski, W. Henley, D. Schielein and J. Lagowski, *J. Elec. Chem. Soc.* **142** 3869, (1995)
10. S. A. McHugo, *Appl. Phys. Lett.* **71**, 1984, (1997)
11. S.A. McHugo, A.C. Thompson, I. Perichaud and S. Martinuzzi, Appl. Phys. Lett., **72**, pg.3482, (1998)
12. I. Périchaud, G. Dour, B. Pillin, F. Durand, D. Sarti and S. Martinuzzi, *Sol. State Phen.* **51-52**, pg. 473, (1996)
13. A.A. MacDowell, R. Celestre, C.H. Chang, K. Franck, M.R. Howells, S. Locklin, H.A. Padmore, J.R. Patel, and R. Sandler, SPIE Proceedings 3152, 126-135 (1998).
14. B. Shen, T. Sekiguchi, R. Zhang, Y. Shi, H. Shi, K. Yang, Y. Zheng and K. Sumino, *Jpn. J. Appl. Phys.* **35**, 3301, (1996)
15. B. Shen, J. Jablonski, T. Sekiguchi and K. Sumino, *Jpn. J. Appl. Phys.* **35**, 4187, (1996)

This work was supported by the Director, Office of Energy Research, Office of Basic Energy Sciences, Materials Sciences Division, of the U.S. Department of Energy, under Contract No. DE-AC03-76SF00098.

Principal investigator: Scott A. McHugo, Advanced Light Source, Ernest Orlando Lawrence Berkeley National Laboratory. Email: samchugo@lbl.gov, Telephone: 510-486-4874.